**INSIGHTS INTO REDOX CYCLING ON EARLY EARTH FROM THE MASS FRACTIONATION LAW OF IRON ISOTOPES IN ARCHEAN SEDIMENTS.** A. W. Heard[1], N. Dauphas[1], O. J. Rouxel[2], N. X. Nie[1], [1]Origins Laboratory, Department of the Geophysical Sciences and Enrico Fermi Institute, The University of Chicago, 5734 South Ellis Avenue, Chicago, IL 60637, United States (andyheard@uchicago.edu), [2]Department of Oceanography, University of Hawaii, Honolulu, HI 96822, United States.

**Introduction:** Iron is an element of great astrobiological interest because of its abundance in planetary surface environments, its multiple redox states, and its processing by microbial metabolisms. The presence of ferric iron in Archean banded iron formations (BIF) indicates that iron oxidation occurred in the surface ocean at a time when the atmosphere and deep ocean on Earth were anoxic. Removal of ferric iron left an imprint on Archean ocean chemistry [1], and deposition of ferric iron on the anoxic sea floor created redox disequilibria ripe for exploitation by microbial life such as through dissimilatory iron respiration (DIR), a metabolism which emerged very early in the history of life on Earth [2-3]. Recent discoveries by the Mars Science Laboratory mission have revealed that an ancient lake in Gale Crater also hosted a redox stratified environment, where Fe (and Mn) oxidized in near surface waters were deposited in disequilibrium with an anoxic lake bottom [4].

Redox processes induce large fractionations in iron isotope ratios, and among BIF and sedimentary pyrites there is a >4‰ variation in $\delta^{56}$Fe of Archean rocks. Removal of isotopically heavy ferric iron oxides to create BIF with positive $\delta^{56}$Fe should have left the Archean ocean with an isotopically depleted ferrous iron reservoir [1]. The case has been made [1] that this depleted reservoir was recorded in shales and sedimentary pyrites, which feature extremely negative $\delta^{56}$Fe. These signatures cannot be, however, uniquely intepreted as reservoir effects because secondary processes, such as kinetic effects during pyrite mineralization [5], or DIR [6], also create isotopically depleted ferrous iron phases. The extent of fractionation in a single iron isotope ratio cannot distinguish between these various processes; but the slope of the mass-fractionation law for two iron isotope ratios, $\delta^{56}$Fe and $\delta^{57}$Fe, may be distinct for different fractionation processes and therefore confirm or deny genetic relationships between different sedimentary reservoirs. We are conducting high-precision triple iron isotope analyses on a suite of Archean sedimentary rocks with a large range of $\delta^{56}$Fe to assess any variation in the mass fractionation law.

**Samples and methods:** BIF samples are from South Africa, Western Australia, Baffin Island and Greenland and span an age range of 3.8 – 2.3 Ga (billion years). Shales and associated pyrites are from 2.63 – 2.32 Ga sedimentary basins in South Africa and Western Australia (all shown in Fig. 1).

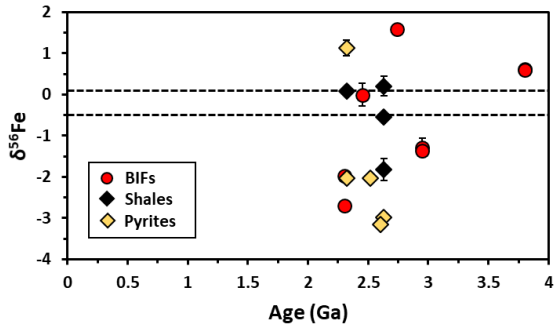


**Figure 1:** Age and iron isotopic composition expressed as $\delta^{56}$Fe of BIF, shale and pyrite samples analyzed in this study. The black dashed lines represent the range of possible initial oceanic values.

Powdered rock samples and whole clean pyrite grains were digested in HF-$HNO_3$-$HClO_4$, then HCl-$HNO_3$-$HClO_4$, and separation of iron was performed on AG1-X8 200-400 mesh Cl-form anion exchange resin using standard [7-8] and long column [9-10] chemistry procedures. Isotopic analyses were made on a Neptune MC-ICPMS in high resolution mode with an Aridus II desolvating nebulizer. Standard-sample bracketing was used and uncertainties are expressed as the 95 % confidence interval of average values. The slope of the mass fractionation law was determined by internal normalization of $^{56}$Fe/$^{54}$Fe to a fixed $^{57}$Fe/$^{54}$Fe along the reference exponential law (Fig. 2).

**Mass fractionation laws:** Mass fractionation laws imparting precise slopes in three-isotope diagrams have previously been studied for O, Mg, S, Ca, Ti, and Fe [9-16], but this has yet to be investigated for Fe isotopes in multiple sedimentary rocks. Mass fractionation laws are straight lines in three-isotope diagrams when the $\delta'$ notation is used:

$$\delta' = 1000 \times \ln\left((\delta/1000)+1\right).$$

The slope $\theta$ for the three-isotope diagram can be parameterized as:

$$\theta^{i1,i2,i3} = \frac{m_{i2}^n - m_{i1}^n}{m_{i3}^n - m_{i1}^n}.$$

where $m_i$ the mass of the isotope i [17]. The value of n characterizes the slope of different mass-dependent fractionation laws.

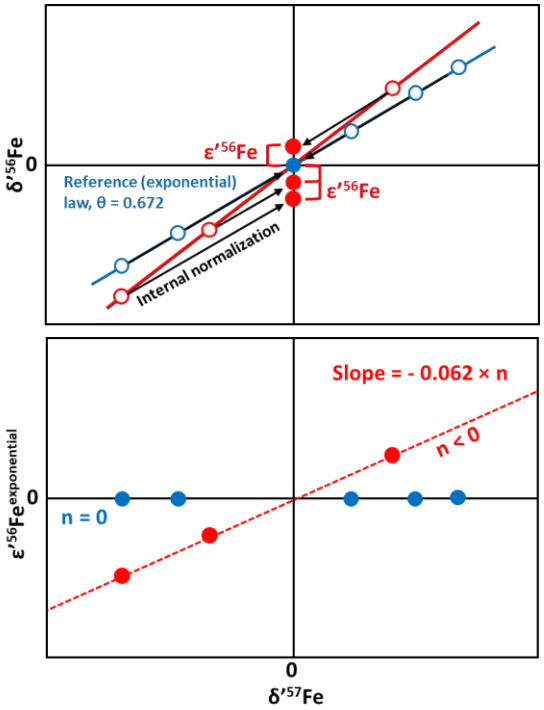


**Figure 2:** *Top.* Illustration of internal normalization of $\delta'^{56}Fe$ values to a fixed $^{57}Fe/^{54}Fe$ along the reference exponential law. Open and closed symbols represent measured and internally normalized values respectively. *Bottom.* Slope of a sample mass fractionation law (red) relative to the reference law (blue) in $\varepsilon'^{56}Fe$ *vs.* $\delta'^{57}Fe$. Slopes are not to scale.

Slopes in three-isotope space vary only subtly, so for visualization purposes one isotope ratio is given as its deviation from the exponential law in parts per $10^4$ by using the $\varepsilon'$ notation (Fig. 2). A Taylor approximation relates the slope of $\varepsilon'$ *vs.* $\delta'$ directly to n, to give the equation for iron isotopes [10]:

$$\varepsilon'^{56}Fe = -0.062 \times n \times \delta'^{57}Fe.$$

Processes that have different iron isotope mass fractionation laws will have different values of n, and thus their products will have distinct $\varepsilon'^{56}Fe$ *vs.* $\delta'^{57}Fe$ slopes.

**Results and conclusions:** High precision data on the mass fractionation law for BIF have been obtained and analysis of shales and pyrites is ongoing. The BIF samples span a range of >4‰ in $\delta^{56}Fe$, with the most isotopically depleted compositions being found in Mn-rich iron formations formed around the time when the terrestrial atmosphere first became oxygenated. The data follow a single mass fractionation line in $\varepsilon'^{56}Fe$ *vs.* $\delta'^{57}Fe$ with a slope of 0.057 ± 0.006, which corresponds to an exponent n = -0.91 ± 0.09. Therefore the BIF mass fractionation law is in agreement with the high-temperature equilibrium limit law (n = -1) and with ferrous and ferric iron reservoirs formed by UV photo-oxidation of aqueous ferrous iron (n = -1.05 ± 0.14) [16]. That process has been proposed to have caused iron oxidation on early Earth [18] and Mars [4,16], and the the hypothesis is consistent with isotopic data from thus study. If Archean shale and pyrite iron isotope signatures passively record the depletion of the oceanic iron reservoir by ferric oxide removal [1], then those samples would follow the same mass fractionation law as BIF. If those samples follow a different mass fractionation law such a result will indicate secondary processes played a major role in their isotopic depletion. Therefore our work will shed light on redox processes in Earth's earliest oceans and possibly biological processes involved in the deposition and reworking of iron-rich chemical sediments.

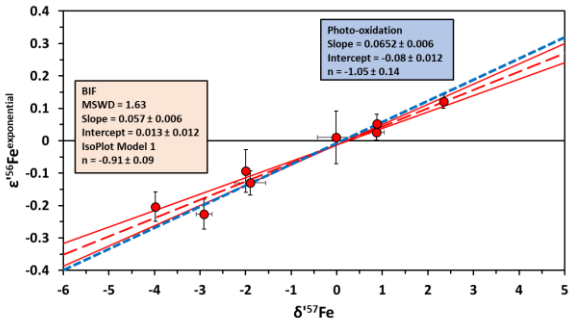


**Figure 3:** Mass fractionation law (red dashed line) for a number of BIF samples (red circles). The slope of the fractionation law is consistent with that found for the UV photo-oxidation process (blue dashed line) [16].

**References:** [1] Rouxel, O. J. *et al.* (2005) *Science, 307,* 1088-1091. [2] Vargas, M. *et al.*(1998) *Nature, 395,* 65-67. [3] Lovley, D. R. (2004) *Origins,* 299–313. [4] Hurowitz, J. A. *et al.* (2017) *Science, 356,* eaah6849. [5] Guilbaud, R. *et al.* (2011) *Science, 332,* 1548–1551. [6] Beard, B. L. *et al.* (1999) *Science, 285,* 1889–1892. [7] Dauphas, N. *et al.* (2004) *Anal. Chem., 76,* 5855–5863. [8] Dauphas, N. *et al.* (2009) *Chem. Geol., 267,* 175–184. [9] Tang, H. *et al.* (2009) *LPS XXXX,* Abstract #1903. [10] Tang, H. and Dauphas, N. (2012) *EPSL, 359–360,* 248–263. [11] Angert, A. *et al.* (2003) *Glob. Biogeochem. Cycles, 17,* 1030. [12] Young *et al.* (2002) *GCA, 66,* 1095-1104. [13] Davis, A. M. *et al.* (2015) *GCA, 158,* 245-261. [14] Farquhar, J. *et al.* (2003) *Geobiology, 1,* 27-36. [15] Zhang, J. *et al.* (2014) *GCA, 140,* 365-380. [16] Nie N. X. *et al.* (2017) *EPSL, 458,* 179-191. [17] Dauphas, N. and Schauble, E. A. (2016) Ann. Rev. Earth Planet. Sci., 44, 709-783 [18] Cairns-Smith, A. G. (1978) *Nature, 276,* 807–808.

**Acknowledgements:** This work was funded by NASA Habitable Worlds (NNH16ZDA001N) Grant 16-HW16_2-0110 to N. Dauphas and A. W. Heard.